GEOPHYSICAL RESEARCH LETTERS, VOL. 35, L21101, doi:10.1029/2008GL035625, 2008

Scale-free and scale-dependent modes of energy release dynamics in the nighttime magnetosphere

V. M. Uritsky,[1] E. Donovan,[1] A. J. Klimas,[2] and E. Spanswick[1]

Received 7 August 2008; revised 3 September 2008; accepted 19 September 2008; published 1 November 2008.

[1] Based on a spatiotemporal analysis of POLAR UVI images, we show for the first time that energy, power, area and lifetime probability distributions of electron precipitation events in the nighttime auroral oval have a significant latitudinal dependence. The low-latitude group of the events contains a distinct subpopulation of strong auroral disturbances violating the uniform power-law behavior reported in previous publications, while the high latitude group is described by nearly perfect power-law statistics over the entire range of scales studied, in agreement with earlier findings. The results obtained indicate that the inner and outer portions of the plasma sheet may be characterized by substantially different scaling regimes of bursty energy dissipation suggestive of different universality classes and/or driving conditions associated with multiscale turbulence in these regions. **Citation:** Uritsky, V. M., E. Donovan, A. J. Klimas, and E. Spanswick (2008), Scale-free and scale-dependent modes of energy release dynamics in the nighttime magnetosphere, *Geophys. Res. Lett.*, *35*, L21101, doi:10.1029/2008GL035625.

1. Introduction

[2] The activity of the nighttime auroral oval represents a wide range of dynamical processes in the magnetotail, including substorm expansion onsets, pseudobreakups, steady magnetospheric convection events with or without substorms, bursty bulk flows, sawtooth events, and other phenomena [see, e.g., *Zesta et al.*, 2000; *Lui*, 2001; *Frey et al.*, 2004; *Henderson et al.*, 2006]. Despite the diversity of physical conditions associated with each particular type of auroral activity, their net energy output can be approximately described by a set of universal power-laws [*Lui et al.*, 2000; *Lui*, 2002; *Uritsky et al.*, 2003, 2002, 2006] signaling the existence of an organizing dynamical principle arranging intermittent magnetospheric dissipation across vast ranges of spatial and temporal scales.

[3] Power-law intermittency of energy dissipation has attracted significant attention in modern statistical mechanics [see *Dhar*, 2006, and references therein] and is often considered a hallmark of turbulent and/or critical phenomena with no characteristic scales other than those dictated by the finite size of the system [*Sreenivasan et al.*, 2004; *Lubeck*, 2004]. Examples of such behavior in geo- and space sciences include fully developed turbulence in hydrodynamic or magnetized flows [*Lazarian*, 2006], Guttenberg-Richter statistics of earthquake magnitudes [*Turcotte*, 1989], scale-invariance in the solar corona [*Charbonneau et al.*, 2001]. In this context, auroral activity provides one of the most impressive examples of scale-free behavior in nature. The energy distribution of electron emission regions exhibits a power-law shape over a range of 6 orders of magnitude [*Uritsky et al.*, 2002]) which can be extended to up to 11 orders by combining satellite data with ground-based TV observations [*Kozelov et al.*, 2004].

[4] The auroral emission statistics reported so far represent global long-term properties of nighttime magnetospheric disturbances. The fact that these properties are dominated by power-law scaling does not eliminate the possibility of a more complex behavior on the level of specific plasma sheet phenomena described by drastically different physical conditions and geometry.

[5] In this study, we are taking a step toward a better understanding of the relationship between the auroral precipitation statistics and the underlying conditions in the central plasma sheet (CPS). The results obtained suggest that the inner and the outer CPS regions are responsible for two distinct scaling modes of energy release dynamics – an essentially scale-free dynamics in the outer CPS, and a more complicated, scale-dependent dissipation in the inner CPS. These results indicate the necessity of a new generation of models of bursty dissipation in the auroral zone incorporating two or more universality classes of the underlying turbulent dynamics.

2. Data and Algorithm

[6] We have studied time series of digital images of nighttime northern aurora (55–80 MLat, 2000–0400 MLT) taken by the Ultraviolet Imager (UVI) onboard the POLAR spacecraft in the 165.5 to 174.5 nm portion of the Lyman-Birge-Hopfield spectral band (integration time 36.5 s, time resolution 184 s). The data analyzed include 16,000 images covering two observation periods: 01/01/1997–02/28/1997 and 01/01/1998–02/28/1998. Our analysis was based on spatiotemporal tracking of auroral emission events [*Uritsky et al.*, 2002, 2003]. The UV luminosity $w(t, \boldsymbol{r})$ was studied as a function of time t and position $\boldsymbol{r}$ on the image plane. First, active auroral regions were identified by applying an activity threshold w_a representing a background UV flux. Contiguous spatial regions with $w(\boldsymbol{r}, t) > w_a$ were treated as pieces of evolving events. Second, by checking for overlap of common pixels between each pair of consecutive UVI frames, we constructed a set of spatiotemporal integration domains $\Lambda_i (i = 1, .., N)$ corresponding to each of N individual emission events found by our method. These domains of contiguous activity in space and time were used

[1]Physics and Astronomy Department, University of Calgary, Calgary, Alberta, Canada.
[2]UMBC at NASA/Goddard Space Flight Center, Greenbelt, Maryland, USA.

0094-8276/08/2008GL035625$05.00

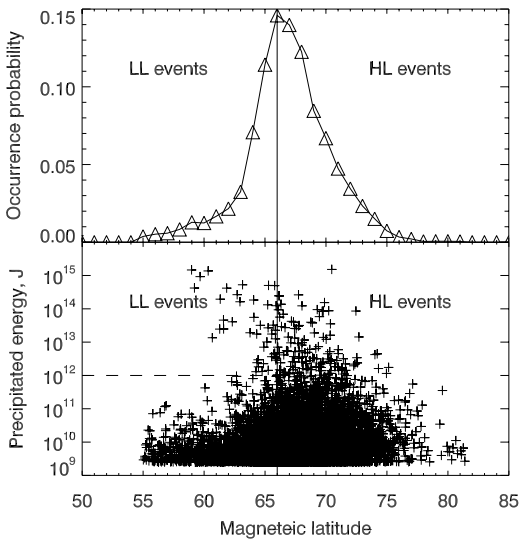

Figure 1. (top) Probability distribution of latitudinal locations of the auroral emission events as defined in the text. (bottom) Scatterplot of emission energies E versus MLAT. The high-latitude (HL) and the low-latitude (LL) events contribute to two distinct scaling regimes of the emission dynamics as shown in Figure 2. The dashed horizontal line marks the position of the energy distribution crossover in Figure 2.

to compute the lifetime, T_i, the energy, $E_i = k \int_{\Lambda_i} w(\boldsymbol{r}, t)\, d\boldsymbol{r}dt$, the peak power, $W_i = k \max_t(\int_{\Lambda_i(t)} w(\boldsymbol{r}, t)\, d\boldsymbol{r})$, as well the peak area, $A_i = \max_t (\int_{\Lambda_i(t)} d\boldsymbol{r})$ of every event, where $k = 2.74 \times 10^{-8}$ J · photon^{-1} [*Brittnacher et al.*, 1997] and the integrals were numerically approximated by sums. The statistics reported below are for the threshold w_a = 10 photons · cm^{-2} · s^{-1}. Their main features remain the same if the threshold is varied at least within the range 5 to 15 photons · cm^{-2} · s^{-1}.

[7] The auroral onset positions of each event were estimated with an error of about 300 km in either spatial direction. We organized the data by the magnetic latitude of the event onset in order to compare the precipitation dynamics that likely originate in the inner CPS relative to dynamics that likely originate in the outer CPS. The populations of the emission events coming from different MLAT ranges were characterized by sets of probability density distributions $p(x)$, where $x \in \{E, W, A, T\}$. The shape of the distributions was quantified by power-law exponents τ_x evaluated using linear regression fitting on the log-log scale, with the subscript indicating the variable under study.

3. Results and Discussion

[8] Figure 1 shows basic statistical features of the entire group (n = 7481) of the emission events detected by our spatiotemporal technique. The probability distribution of the event magnetic latitude (Figure 1, top) has a sharp peak at ~66° MLAT. In the subsequent discussion, the events that initiate to the left and to the right of this peak are denoted respectively as low-latitude (LL) and high-latitude (HL) events. We note that the distribution in Figure 1 includes all possible types of precipitation activity in the studied auroral sector and is not to be directly compared with substorm onset distributions. Figure 1 (bottom) shows the emission energy E as a function of event latitude. Both plots have an asymmetric shape suggesting different statistics for the LL and HL events. We have found that these statistical subsets

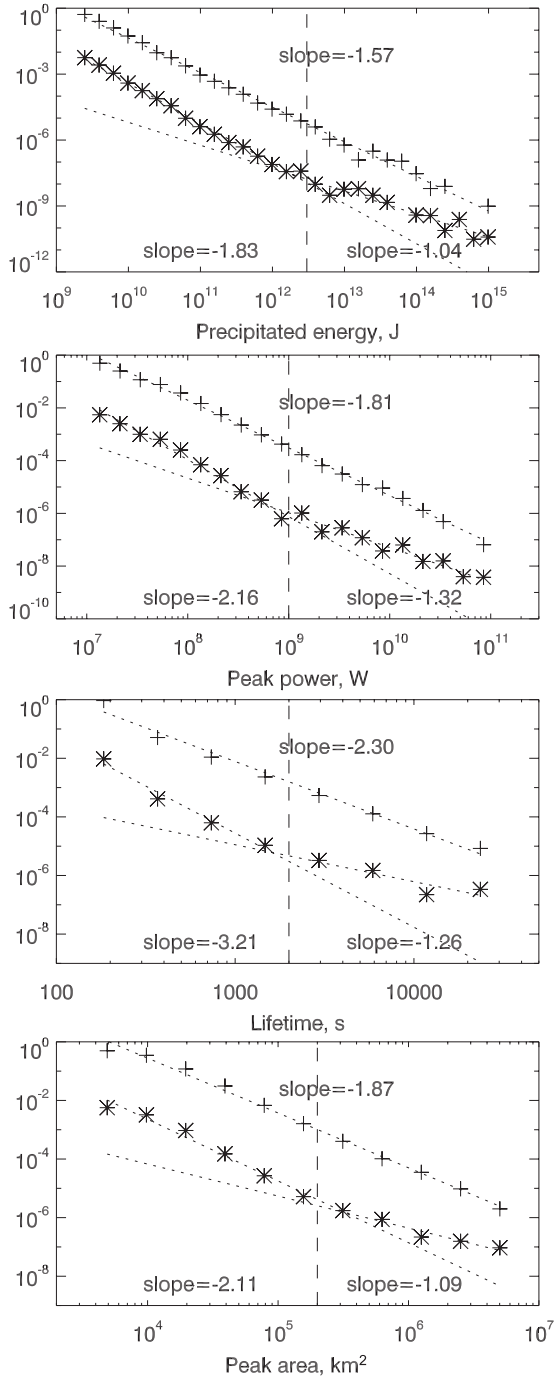

Figure 2. Probability distributions of energy E, peak power W, lifetime T, and peak area A of auroral emission events belonging to HL (crosses) and LL (stars) populations. The low-latitude distributions are shifted downward for easier comparison. The dotted lines show the log-log distribution slopes for small- and large-scale LL events measured to the left and to the right of the dashed vertical lines marking the crossovers, as well as for the entire HL population.

Table 1. Power-Law Distribution Exponents of High-Latitude and Low-Latitude Emission Events[a]

	HL	LL(s)	LL(l)	C
$p(E)$	1.57 ± 0.02	1.83 ± 0.04	1.04 ± 0.12	3×10^{12} J
	(n = 5204)	(n = 2242)	(n = 35)	
$p(W)$	1.81 ± 0.02	2.16 ± 0.09	1.32 ± 0.14	1×10^{9} W
	(n = 5204)	(n = 2219)	(n = 58)	
$p(T)$	2.30 ± 0.11	3.21 ± 0.33	1.26 ± 0.44	2×10^{3} s
	(n = 5204)	(n = 2232)	(n = 45)	
$p(A)$	1.87 ± 0.05	2.11 ± 0.16	1.09 ± 0.14	2×10^{5} km^2
	(n = 5204)	(n = 2208)	(n = 69)	

[a]The approximate value of the crossover C is given for each distribution. HL is high-latitude emission events, LL is low-latitude emission events, s is small-scale portion, and l is large-scale portion of the LL distributions in Figure 2.

are characterized by significantly different regimes of scaling behavior.

[9] Figure 2 shows probability distributions for LL and HL events. The HL population exhibits stable power-law distributions of emission energy E, peak emission power W, lifetime T and peak area A with low regression errors (see Table 1). These power-law behaviors involve both small auroral activations and large events whose energy output lie in the range of global substorms according to *Carbary et al.* [2000].

[10] The LL events have more complicated statistical properties, as could be expected from the energy scatterplot in Figure 1. The distribution functions of these events demonstrate a distinct crossover behavior involving small-scale regions described by distribution exponents which are significantly greater than the corresponding exponents of HL events, as well as large-scale regions where the slopes are significantly shallower. The position of the energy crossover $E \approx 3 \times 10^{12}$ J in the $p(E)$ distribution is in agreement with the data gap in Figure 1 (bottom) separating low- and high-energy LL events.

[11] Figure 3 provides further insight into the latitudinal behavior of the scaling exponents. Here, the entire range of magnetic latitudes covered by our analysis was divided into four subranges, each containing roughly the same number of data points. In each latitudinal subrange, the exponents were evaluated both below and above the distribution crossovers. It can be seen that at low latitudes, the large- and small-scale exponents are significantly different. However, as the latitude increases, this difference tends to be less and less significant. For three out of four emission parameters (W, T and A), the distribution exponent values below and above the crossover become statistically indistinguishable at MLAT $\geq 67°$. This analysis indicates that the emission dynamics undergoes a gradual transition from scale-dependent to scale-free modes with the increase of the event latitude, possibly reflecting mapping variability in different magnetotail configurations.

[12] The mean values and standard errors of the scaling exponents as well as the approximate positions of the distribution crossovers are summarized in Table 1. The error analysis confirms that the scaling behaviors of the LL and LH events are described by substantially different sets of τ_x values.

[13] According to our estimates, about 2/3 of the detected emission events contribute to the scale-free HL population.

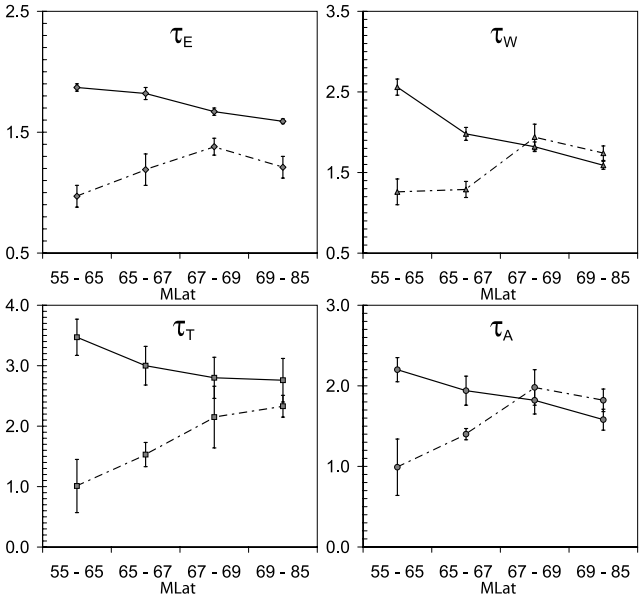

Figure 3. Large-scale (solid lines) and small-scale (dot-dashed lines) probability distribution exponents for several latitudinal subranges. Vertical bars show standard linear regression errors for each measurement. Note that the differences between the large- and small-scale exponents decrease as the MLAT increases.

The HL exponents are quite close to the values obtained earlier for the same observation period without filtering the activity by the event location [*Uritsky et al.*, 2002, 2003]. Therefore, in the statistical sense, the scale-free mode dominates the behavior of the nighttime auroral oval. On the other hand, despite its lower relative occurrence, the scale-dependent LL activity plays a prevailing role in the energy budget of the nighttime electron aurora. Indeed, the total precipitation energy $E_{tot} = \sum E_i$ released by these events approaches 70 percent of the overall energy. Interestingly, a substantial portion of this energy can be ascribed to auroral breakups which initiate in the equatorward part of the auroral zone.

[14] Table 2 contains several additional parameters reflecting the state of the solar wind and the auroral magnetosphere at the beginnings of emission events. The data show that the LL events are characterized by significantly higher statistical values of solar wind dynamic pressure and elec-

Table 2. Average Values of the Event Magnetic Latitude, Total Emission Energy, Solar Wind Dynamic Pressure, Auroral Electrojet Index, and the Magnetotail Index Proxy for the Two Populations of the Emission Events[a]

	HL	LL (all)
Event MLAT, deg	69.06 ± 0.03	63.58 ± 0.05
E_{tot}, J $\times 10^{15}$	4.3 ± 1.6	7.7 ± 2.5
P_d, nPa	2.54 ± 0.02	2.76 ± 0.03
AE, nT	135 ± 2	228 ± 4
MT index, deg	63.68 ± 0.02	63.12 ± 0.03

[a]E_{tot} is total emission energy, P_d is solar wind dynamic pressure, AE is the auroral electrojet index, and MT index is the magnetotail index proxy [*Gvozdevsky and Sergeev*, 1995].

trojet index as compared to the HL population. Also, the LL events seem to appear in a more stretched magnetotail configuration as reflected by the lower value of the magnetotail (MT) index proxy [*Gvozdevsky and Sergeev*, 1995] based on hourly AE index and solar wind dynamic pressure values. It should be added that any statistical relationship such as the ones used for computing this proxy strongly underestimates the magnetic field stretching near the time of the substorm onset, meaning that the real MT index of large-scale LL events should be even smaller.

[15] On the whole, the data suggest that the scale-dependent mode of auroral precipitation dynamics is associated with a more unstable state of the CPS (higher geomagnetic activity level, stronger solar wind driving, less dipolar magnetic field) as compared to the scale-free mode.

[16] Judging by their average MLAT location, the HL events should mainly initiate in the outer CPS region. The energy conversion in this region is believed to be dominated by magnetic reconnection [*Birn and Hones*, 1981]. The power-law emission exponents that we have found in this region are rather close to the exponents from a driven current sheet simulation [*Klimas et al.*, 2004] consistent with multiscale turbulent reconnection being the source of scale-invariance in the outer CPS dynamics. This agreement supports the conjecture that the near-Earth (midtail) reconnection is a turbulent bursty process with no well-defined dissipation scales. However, strong precipitation events in the high-latitude region are known to involve considerable field-aligned acceleration in the upper ionosphere, and the statistics of the HL population can be strongly modulated by this process. This influence requires careful analysis which is beyond the scope of this study.

[17] The substorm-scale LL events are likely to be produced in the inner part of the plasma sheet which is not a region that favors magnetic reconnection. However, this region can be prone to current disruption which offers an alternate mechanism for energy release in the inner tail [*Lui*, 2000]. The small-scale LL events can be attributed to mostly diffuse auroral forms at the latitudes below the proton isotropic boundary and are therefore generated in the inner magnetosphere.

[18] Our main new result concerns the low-latitude auroral region, where two different populations, small-scale emission events with unusually steep distributions slopes and rare high-energy events with much shallower slopes were detected. The high-latitude emission events are found to follow broad-band power-law statistics with no characteristic scales.

[19] The existence of two or more scaling regimes within the same physical system may signal the presence of several distinct universality classes (UC) responsible for the observed turbulent dynamics [*Lubeck*, 2004; *Dhar*, 2006]. It is known that many stochastic scale-invariant phenomena can be mapped onto a finite collection of such classes. Typically, each UC brings its own set of critical exponents which express its inherent set of relevant variables and the underlying symmetries (dynamic invariants) [*BenHur and Biham*, 1996] Our results suggest that although the energy release dynamics in the magnetosphere is predominantly scale-free, it can not be accurately described in terms of a single UC as was proposed before [see, e.g., *Chapman et al.*, 1999; *Uritsky and Pudovkin*, 1998; *Consolini*, 2002], and involves a substantially more complicated interplay between a variety of dissipation mechanisms in the CPS modulated by the solar wind driver and the magnetosphere-ionosphere coupling.

[20] **Acknowledgments.** This work was partly supported by NSERC operating grant of EFD. We thank William Liu for stimulating discussions, Art Richmond for APEX conversion algorithms, and George Parks and Daniel Chua for calibrated POLAR UVI data.

References

BenHur, A., and O. Biham (1996), Universality in sandpile models, *Phys. Rev. E*, *53*(2), R1317–R1320.

Birn, J., and E. W. Hones (1981), Three-dimensional computer modeling of dynamic reconnection in the geomagnetic tail, *J. Geophys. Res.*, *86*(A8), 6802–6808.

Brittnacher, M., R. Elsen, G. Parks, L. Chen, G. Germany, and J. Spann (1997), A dayside auroral energy deposition case study using the POLAR Ultraviolet imager, *Geophys. Res. Lett.*, *24*(8), 991–994.

Carbary, J. F., K. Liou, A. T. Y. Lui, P. T. Newell, and C. I. Meng (2000), "Blob" analysis of auroral substorm dynamics, *J. Geophys. Res.*, *105*(A7), 16,083–16,091.

Chapman, S. C., R. O. Dendy, and G. Rowlands (1999), A sandpile model with dual scaling regimes for laboratory, space and astrophysical plasmas, *Phys. Plasmas*, *6*(11), 4169–4177.

Charbonneau, P., S. W. McIntosh, H. L. Liu, and T. J. Bogdan (2001), Avalanche models for solar flares, *Solar Phys.*, *203*(2), 321–353.

Consolini, G. (2002), Self-organized criticality: A new paradigm for the magnetotail dynamics, *Fractals*, *10*(3), 275–283.

Dhar, D. (2006), Theoretical studies of self-organized criticality, *Physica A*, *369*(1), 29–70.

Frey, H. U., S. B. Mende, V. Angelopoulos, and E. F. Donovan (2004), Substorm onset observations by IMAGE-FUV, *J. Geophys. Res.*, *109*, A10304, doi:10.1029/2004JA010607.

Gvozdevsky, B. B., and V. A. Sergeev (1995), MT-index—A possible new index to characterize the configuration of the magnetotail, *Adv. Space Res.*, *18*(8), 51–54.

Henderson, M. G., et al. (2006), Substorms during the 10–11 August 2000 sawtooth event, *J. Geophys. Res.*, *111*, A06206, doi:10.1029/2005JA011366.

Klimas, A. J., V. M. Uritsky, D. Vassiliadis, and D. N. Baker (2004), Reconnection and scale-free avalanching in a driven current-sheet model, *J. Geophys. Res.*, *109*, A02218, doi:10.1029/2003JA010036.

Kozelov, B. V., V. M. Uritsky, and A. J. Klimas (2004), Power law probability distributions of multiscale auroral dynamics from ground-based TV observations, *Geophys. Res. Lett.*, *31*, L20804, doi:10.1029/2004GL020962.

Lazarian, A. (2006), Intermittency of magnetohydrodynamic turbulence: An astrophysical perspective, *Int. J. Mod. Phys. D*, *15*(7), 1099–1111.

Lubeck, S. (2004), Universal scaling behavior of non-equilibrium phase transitions, *Int. J. Mod. Phys. B*, *18*(31–32), 3977–4118.

Lui, A. T. Y. (2000), Electric current approach to magnetospheric dynamics and the distinction between current disruption and magnetic reconnection, in *Magnetospheric Current Systems*, *Geophys. Monogr. Ser.*, vol. 118, edited by S. Ohtani et al., pp. 31–40, AGU, Washington, D. C.

Lui, A. T. Y. (2001), Current controversies in magnetospheric physics, *Rev. Geophys.*, *39*(4), 535–563.

Lui, A. T. Y. (2002), Multiscale phenomena in the near-Earth magnetosphere, *J. Atmos. Sol. Terr. Phys.*, *64*(2), 125–143.

Lui, A. T. Y., S. C. Chapman, K. Liou, P. T. Newell, C. I. Meng, M. Brittnacher, and G. K. Parks (2000), Is the dynamic magnetosphere an avalanching system?, *Geophys. Res. Lett.*, *27*(7), 911–914.

Sreenivasan, K. R., A. Bershadskii, and J. J. Niemela (2004), Multiscale SOC in turbulent convection, *Physica A*, *340*(4), 574–579.

Turcotte, D. L. (1989), Fractals in geology and geophysics, *Pure Appl. Geophys.*, *131*(1–2), 171–196.

Uritsky, V. M., and M. I. Pudovkin (1998), Low frequency 1/*f*-like fluctuations of the AE-index as a possible manifestation of self-organized criticality in the magnetosphere, *Ann. Geophys.*, *16*(12), 1580–1588.

Uritsky, V. M., A. J. Klimas, D. Vassiliadis, D. Chua, and G. Parks (2002), Scale-free statistics of spatiotemporal auroral emissions as depicted by POLAR UVI images: Dynamic magnetosphere is an avalanching system, *J. Geophys. Res.*, *107*(A12), 1426, doi:10.1029/2001JA000281.

Uritsky, V. M., A. J. Klimas, and D. Vassiliadis (2003), Evaluation of spreading critical exponents from the spatiotemporal evolution of emission regions in the nighttime aurora, *Geophys. Res. Lett.*, *30*(15), 1813, doi:10.1029/2002GL016556.

Uritsky, V. M., A. J. Klimas, and D. Vassiliadis (2006), Critical finite-size scaling of energy and lifetime probability distributions of auroral emissions, *Geophys. Res. Lett.*, *33*, L08102, doi:10.1029/2005GL025330.

Zesta, E., L. R. Lyons, and E. Donovan (2000), The auroral signature of earthward flow bursts observed in the magnetotail, *Geophys. Res. Lett.*, *27*(20), 3241–3244.

E. Donovan, E. Spanswick, and V. M. Uritsky, Physics and Astronomy Department, University of Calgary, SB605, 2500 University Drive NW, Calgary, AB T3A 0P4, Canada. (vuritsky@phas.ucalgary.ca)

A. J. Klimas, UMBC at NASA/Goddard Space Flight Center, Mail Code 692, Greenbelt, MD 20771, USA.